ELSEVIER

European Journal of Cardio-thoracic Surgery 37 (2010) 384—392

EUROPEAN JOURNAL OF CARDIO-THORACIC SURGERY

www.elsevier.com/locate/ejcts

The architecture of the left ventricular myocytes relative to left ventricular systolic function

Farshad Dorri [a], Peter F. Niederer [a,*], Paul P. Lunkenheimer [b], Robert H. Anderson [c]

[a] *Institute of Biomedical Engineering, University and ETH Zurich, Gloriastrasse 35, CH-8092 Zurich, Switzerland*
[b] *Experimental Thoracovascular and Cardiac Surgery, University of Munster, Domagkstrasse 11, 48149 Munster, Germany*
[c] *Cardiac Unit, Institute of Child Health, University College, London, UK*

Received 16 February 2009; received in revised form 6 July 2009; accepted 8 July 2009; Available online 29 August 2009

Abstract

Objective: Mural thickening, combined with longitudinal and circumferential shortening, and apical along with basal twisting are critical components of the left ventricular systolic deformation that contribute to ventricular ejection. It is axiomatic that the spatial alignment of the actively contracting aggregates of myocytes must play a major role in the resulting ventricular deformation. The need to conserve functional global myocytic architecture, therefore, is an important aspect of the surgical manoeuvres affecting ventricular mass and geometry. To investigate the influence of the global alignment of the myocytes on ventricular contraction, we used a mathematical model simulating the large deformations produced by systolic contraction of the left ventricle of a human heart. **Methods:** The alignment and meshing of the myocytes within their supporting fibrous matrix cause mechanical anisotropy, which was included in the mathematical model in the form of a unit vector field, constructed from the measured trajectories of aggregated myocytes in an autopsied human heart. The relationship between ventricular structure and ventricular dynamics was assessed by analysing the influence of systematic deviations of the orientation of the myocytes from their original alignment, in longitudinal as well as radial directions, on the distribution of stress and strain within the myocardium, as well as on the ejection fraction. In addition, simplified idealised geometries were used to investigate the influence of the overall geometrical modifications. **Results:** Left ventricular function proved to be robust with respect to small-to-moderate rotational variations in myocytic alignment, up to 14°, a finding which we attribute to an equalising effect of the non-uniform anisotropic pattern found in a real heart involving substantial local irregularities in the architecture of the aggregated myocytes. Severe deterioration of function occurred only when deviations in alignment exceeded 30°. **Conclusions:** Our findings substantiate the concept of the myocardial walls representing a continuous three-dimensional meshwork, with the absence of any intermediate structures such as discrete bands or tracts extending over the ventricles, which could be destroyed surgically, thereby adversely affecting systolic function. With appropriate indications, they also support the validity of the surgical procedures performed to reduce ventricular radius and therefore to reduce mural stress.
© 2009 European Association for Cardio-Thoracic Surgery. Published by Elsevier B.V. All rights reserved.

Keywords: Heart; Myocardium; Contraction; Anisotropy; Fibre orientation

1. Introduction

The human ventricular walls are made up of well-aligned and multiply branching myocytes, anchored by a dense collageneous matrix [1—3]. Although there is a considerable regional variability in the orientation of the individual myocytes, an overall longitudinal alignment of myocytic aggregates can readily be discerned. Within the walls, moreover, there are numerous short gaps, where there is very limited branching between the adjacent chains of aggregated myocytes. The dimension, orientation and location of these gaps vary greatly. They are assumed to facilitate the relative movement of the aggregated chains of myocytes during systolic contraction, such rearrangement being held necessary to explain the full extent of systolic mural thickening [4].

While the essentially uniaxial orientation of the aggregated myocytes is well seen in histological preparations, the overall global ventricular mural architecture is more difficult to assess. In the past, there has been a tendency to extrapolate from the observations on selected regions to provide an overview of the global ventricular structure. It is also difficult to infer three-dimensional (3D) spatial structure from planar microscopic views. Based on the available evidence from histological methods [1,2], peeling procedures [5] and non-invasive imaging [6,7], our working hypothesis is that, from a mechanical point of view, the ventricular walls are made up of myocytes that merge in an anisotropic fashion with their neighbours to form almost endless trajectories — the overall effect being to produce a

* Corresponding author. Tel.: +41 44 632 4568; fax: +41 44 632 1193.
E-mail address: niederer@biomed.ee.ethz.ch (P.F. Niederer).

1010-7940/$ — see front matter © 2009 European Association for Cardio-Thoracic Surgery. Published by Elsevier B.V. All rights reserved.
doi:10.1016/j.ejcts.2009.07.010

Downloaded from https://academic.oup.com/ejcts/article/37/2/384/775894 by guest on 25 April 2024

unitary and continuous meshwork of myocytes contained within a collageneous matrix.

Within the epicardial and endocardial components of the ventricular wall, the aggregated myocytes are mostly aligned in a surface-parallel fashion, being orientated as helical forms. Assessment at increasing depths within the wall reveals a gradation in helical angulation, whereby the angle varies from −80°, when assessed relative to the equatorial plane and viewed in clockwise direction at the epicardium, to +80° at the endocardial surface. The mid-portion of the ventricular wall is made up primarily of myocytes aggregated together in a circumferential fashion [1,2]. In addition, however, an important population of myocytes is aggregated to intrude obliquely between superjacent aggregates [5,8]. To date, those investigators producing models to explain ventricular function have largely ignored these myocytes, yet the intruding population has been shown to produce important auxotonic forces during ventricular contraction [9].

Ignoring the intruding myocytes could prove significant, in particular as theoretical considerations regarding cardiac output have been based on the so-called optimal myocytic architecture [10]. In reality, there are marked local inhomogeneities in the 3D meshwork, which deviates significantly from such a presumed uniform and allegedly optimal structure. It is our belief that such deviations play significant roles in cardiodynamics, serving to regularise overall contraction, maintain it within non-self-destructing limits and ensuring that the ventricles can function within a large range of anatomical and physiological conditions [9,11].

Some authors seeking to explain cardiodynamics have presumed the presence of discrete and sizable anatomical subcomponents making up and extending in a coherent fashion over the ventricular walls, describing these parts in terms of tracts, spirals, layers or bands [12,13]. Yet, to the best of our knowledge, such structures have never been demonstrated histologically, nor are they necessary for a physiologic ventricular contraction [14]. We doubt, in particular, whether the pronounced local heterogeneities in the myocytic orientation are compatible with notions of well-defined, coherent and dissectable subcomponents extending over the ventricles. If the myocardium was truly composed of discrete and sizable substructures of cardiodynamic significance, we would expect that surgical manoeuvres that changed the ventricular architecture would be deleterious for systolic function, since such procedures would break up the purported ventricle-wide subunits. This would occur, for example, in surgical procedures designed to reduce the ventricular radius, where significant amounts of contractile myocardium are resected with the aim of reducing mural stress. Associated with this procedure, which may lead to a substantially improved ventricular function, is, among others, a pronounced reorientation of the myocytes aggregated within the ventricular walls. It is the individual myocyte that is the basic active myocardial unit with the aggregated myocytes arranged in an essentially continuous fashion; we now expect that small-to-moderate variations in the mural architecture exert only moderate influences on cardiac performance. To test this hypothesis, we conducted a number of numerical simulations based on the architecture of a healthy human left ventricle, in which we had already determined the alignment of the aggregated myocytes by the technique of peeling [5]. Using these anatomical data, we first simulated systematic alterations in the alignment of the aggregated myocytes assessing their influence on selected, albeit representative, indicators of cardiodynamics such as stroke volume, stress and strain. To investigate the influence of geometry on global ventricular function and to exclude eventual incidental influences due to the particular configuration of the myocytes within the chosen heart, we made further changes in the shape and size of the model.

2. Methods

2.1. Anatomical model

We performed the simulations using a finite element (FE) model of an autopsied healthy human heart as described and validated previously [14]. Its shape and internal anisotropic structure (Fig. 1a and b) were defined with the aid of a unit vector field, $\vec{N}$, which characterised the spatial orientation of the aggregated myocytes throughout the ventricular mass and which was obtained by peeling a representative human ventricle. As a constitutive model, we extended the orthotropic material law proposed by Lin and Yin [15], whereby systolic contraction was modelled by the addition of active components to the stress tensor. We used some 46 000 elements, with a typical edge length of around 1 mm, to model the left ventricular wall.

Those readers who are not interested in the further mathematical procedures are advised to skip the two sections of the text which follow and to proceed directly to the section entitled 'Structural variation of the left ventricle'.

2.2. Constitutive properties of the myocardium

The material characteristics of the myocardium, containing passive and active components, were approximated as strands of active, contractile material embedded in a passive, homogeneous and isotropic matrix. This simplification enabled us to deduce an appropriate form of the orthotropic strain energy function [15–17] directly from the experimental data [16,18].

The strain energy function of the passive component, W_{pass}, consisted of an incompressible part, W_{inc} and a volumetric contribution W_{vol}:

$$W_{pass} = W_{inc} + W_{vol} \quad (1)$$

With the right Cauchy–Green deformation tensor, $\boldsymbol{C}$, the material constants c_0, c_5 and the invariants

$$I_1 = \mathrm{tr}(\boldsymbol{C})$$
$$I_2 = 1/2\left[(\mathrm{tr}\boldsymbol{C})^2 - \mathrm{tr}\boldsymbol{C}^2\right]$$
$$I_3 = 1(\text{incompressibility})$$
$$I_4 = \vec{\mathrm{N}} \cdot \boldsymbol{C} \cdot \vec{\mathrm{N}}$$

Downloaded from https://academic.oup.com/ejcts/article/37/2/384/775894 by guest on 25 April 2024

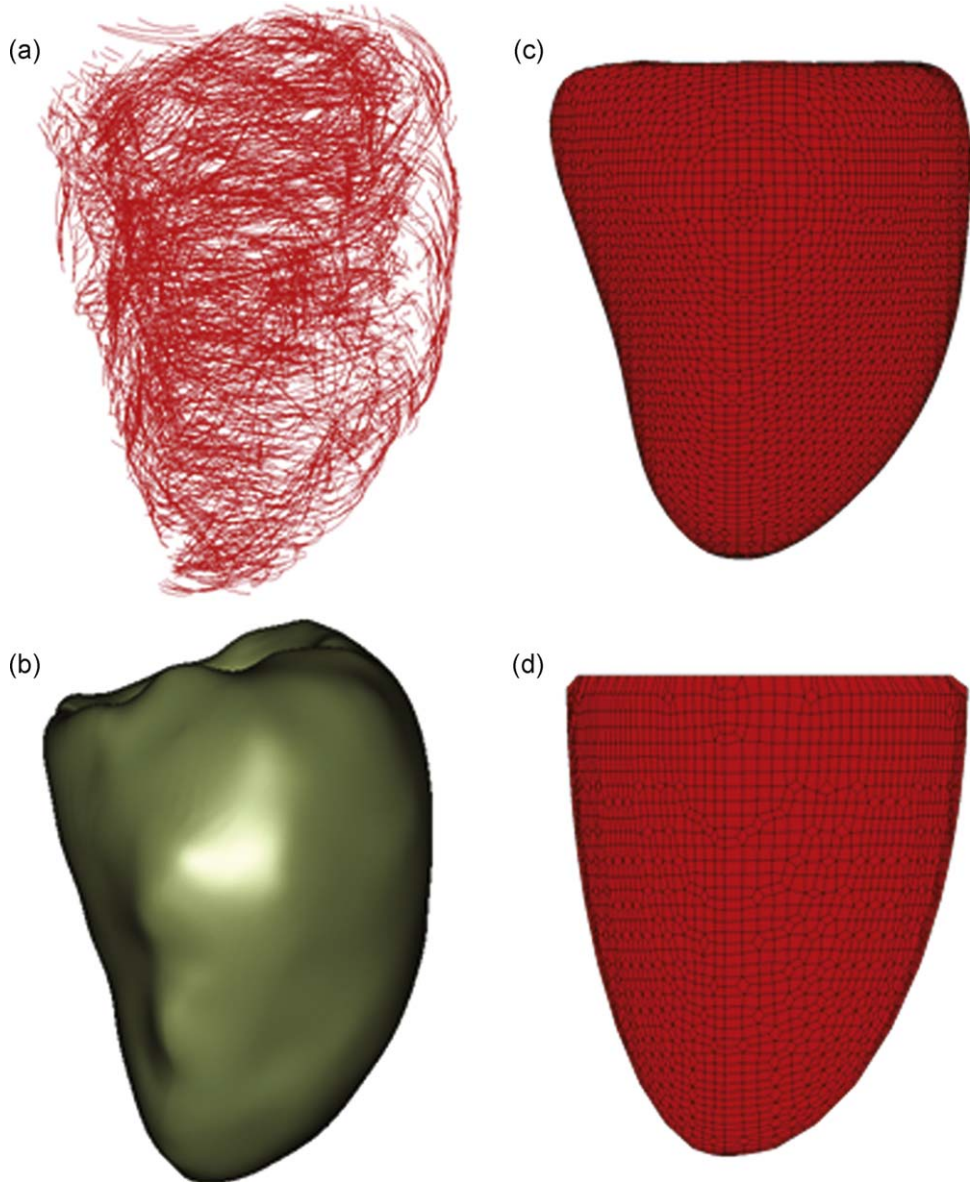

Fig. 1. Panel *a* shows the trajectories of myocytes within the left ventricle approximated as cubic splines from the digitised points outlining the aggregated myocytes Panel *b* is a geometrical model of the human left ventricle. The corresponding FE model contains about 46 000 eight-node hexahedral elements (the typical edge length is around 1 mm). Panel *c* shows the mesh of a truncated geometry of the left ventricle with 19 600 elements constructed from the point clouds representing the endocardial and epicardial surfaces of a representative autopsied human heart. Panel *d* shows the mesh of the adjusted spheroidal geometry of the left ventricle with 11 700 elements.

the function for the incompressible part reads

$$W_{\text{inc}} = c_0 + c_1(I_1 - 3)(I_4 - 1) + c_2(I_1 - 3)^2 + c_3(I_4 - 1)^2 + c_4(I_1 - 3) + c_5(I_4 - 1) \quad (2)$$

The material parameters (in g cm^{-3}) were chosen as $c_0 = 0$, $c_1 = -7.89$, $c_2 = 66.2$, $c_3 = 51.12$, $c_4 = 40.12$ and $c_5 = 0.0032$.

An effective compressibility of the tissue was taken into account by the volumetric contribution:

$$W_{\text{vol}} = \frac{9\kappa}{2}(J - 1)^{1/3} \quad (3)$$

where $J = \sqrt{det(\boldsymbol{C})}$ and the modulus $\kappa = 70$ kPa. This value corresponds to a relatively high compressibility, exceeding the one reported in the literature [16]. Apart from some compressibility due to interstitial fluid flow, the rearrangement of the myocytes during systole manifests itself formally as virtual or pseudo-compressibility within the framework of our model, since the constitutive formulation (Eq. (1)) does not reflect the effect of the numerous small gaps within the myocardial mass. These gaps whose function cannot be implemented in a constitutive model straightforwardly are assumed to enhance wall thickening by allowing relative displacements of the strains associated with myocytes.

Besides a global rectangular coordinate system (x, y, z) with unit vectors $\{\vec{e}_i\}$ ($\vec{e}_3$ along the long axis of the ventricle, the other two components being perpendicular to that axis), we defined a local rectangular coordinate system (x'_{Fi}, y'_{Si},

Downloaded from https://academic.oup.com/ejcts/article/37/2/384/775894 by guest on 25 April 2024

z'_{Ni}) with unit vectors $\{\vec{e}'_i\}$ for each finite element, i, whereby the x'_{Fi} direction was given by the orthotropy, y'_{Si} perpendicular to this direction and perpendicular to the ventricular long axis and z'_{Ni} completing the rectangular system.

Systolic contraction was modelled by defining the total second Piola–Kirchhoff stress tensor $\boldsymbol{S}$ as the sum of a passive part, $\boldsymbol{S}_{passive}$, derived from the relation according to Eq. (1) and an active contribution, $\boldsymbol{S}_{active}$, defined and increased at each integration step (see below).

The active contribution was applied in every finite element, denoted by prime, and included the longitudinal, the cross-cellular forces as well as the shear between the strands of myocytes.

$$\boldsymbol{S}'_{active} = \begin{pmatrix} S'_{active}(F,F) & 0 & 0 \\ 0 & 0 & S'_{active}(S,N) \\ 0 & S'_{active}(N,S) & S'_{active}(N,N) \end{pmatrix} \quad (4)$$

Therefore, the indices S, F and N correspond to the local axes x'_{Fi}, y'_{Si} and z'_{Ni}. We assumed that Eq. (4) was equal for all elements. Before the calculation, all local contributions (denoted by prime) were transformed to the global system.

2.3. Boundary conditions

A uniform left ventricular intracavitary blood pressure curve,

$$p_{LV} = -944t^2 + 245t \quad 0 \le t \le 0.2\,\text{s}$$

was applied as the boundary condition, representing a formal intracavital pressure curve with a maximum of 16 kPa at time t = 0.13 s. In turn, the systolic pressure in the right ventricle acting on the septum was approximated by a correspondingly scaled curve with a maximum of 4 kPa. Although we did not explicitly include the right ventricle in our model, the intracavitary pressure in this ventricle was needed as a boundary condition along the septal region. Intracavital pressure gradients, which are less than 1 kPa, typically, were neglected within the approximations and accuracy of our simulations. Similarly, eventual end-diastolic residual stresses were not considered since they are small in comparison with systolic wall stresses.

The time, t, is of a virtual nature in our model, since inertial and viscous effects were not considered because these effects can again be disregarded within the framework of our (hence, quasi-static) approximations. The parameter was, however, used to parameterise the systolic contraction, which was modelled in a stepwise fashion. Starting with intracavital pressure zero, a first increment of the active stress tensor

$$\boldsymbol{S}'_{active}\text{inc} = \begin{pmatrix} 3 & 0 & 0 \\ 0 & 0 & 0.1 \\ 0 & 0.1 & 1.8 \end{pmatrix}$$

was applied in every finite element. This choice implied that the value of $S'_{active}(N,N)$ was 60% of $S'_{active}(F,F)$, which is consistent with previous biaxial experiments [19]. The value of $S'_{active}(S,N)$ was, furthermore, about 3% of $S'_{active}(F,F)$. In this fashion, the natural sequence of events, that is, the onset of active systolic wall stress followed by intracavital pressure increase was mimicked.

To enable execution of the integration step, the intracavital pressure had to be described as a boundary condition. Since the intracavital pressure increment corresponding to the given stress increment was not known *a priori*, it was estimated. This did not usually lead to an equilibrium state. Accordingly, the intracavital pressure increment was varied along the prescribed pressure curve iteratively until a quasi-static equilibrium involving wall stresses, geometry and intracavital pressure was reached. The same active stress increment was consecutively used whereby the intracavital pressure increase was determined each time as described by iteration. The calculation was terminated when the pressure reached its prescribed maximum. The simulated stroke volume was calculated from the ventricular volumes at the beginning and at the end of the simulation.

2.4. Structural variation of the left ventricle

First, we imposed uniform variations of the orientation field on each element of the finite element mesh to investigate the impact of changes of orientation of the aggregated myocytes on the systolic left ventricular function. Ventricular geometry and boundary conditions were kept unchanged. Second, three different geometrical models were used to ascertain that the overall results were not associated with the particular geometry of the human heart used to establish the myocardial architecture.

To vary the orientation field, we transformed the local rectangular coordinate system, defined above for each finite element, namely x'_{Fi} (direction of orthotropy, given by the vector field $\vec{N}$), y'_{Si} (radial direction and perpendicular to the direction of x'_{Fi}) and z'_{Ni} (perpendicular to both the previous ones) prior to each simulation. This was achieved by the application of rotation matrices $\boldsymbol{\Phi}(\phi)$, $\boldsymbol{\Theta}(\theta)$ and $\boldsymbol{\Omega}(\omega)$ providing rotations around the three axes z'_{Ni} (variation of angle of intrusion), y'_{Si} (variation of helical angle) and x'_{Fi} (variation around direction of orthotropy), respectively. Equal steps Δ of $\pm 2^\circ$ for $\Delta\phi$, $\Delta\theta$ and $\Delta\omega$ each were sequentially applied to each rotation up to a maximal value of $\pm 14^\circ$ for ϕ, θ and ω each. Therefore, negative angles denoted a clockwise turn and positive ones a counter clockwise turn when viewed in the positive coordinate direction.

To complete the investigation and analyse the influence of directional variations larger than 14°, we introduced rotations of up to 90°.

2.5. Left ventricular conformational variations

Third, in order to compare the impact of geometrical details on left ventricular systolic contraction, we used two other models, which were modified from the original geometry (Fig. 1c and d; keeping the same end-diastolic volume of 118 ml). In all simulations, we applied the same constitutive equation, material parameters and boundary conditions. The direction field, $\vec{N}$, was interpolated and adapted to the various geometries such that the models possessed a similar anisotropic architecture.

In the modification according to Fig. 1c, the original model was truncated at the base and a new FE mesh consisting of

Downloaded from https://academic.oup.com/ejcts/article/37/2/384/775894 by guest on 25 April 2024

some 19 600 elements was constructed. In a further step, the left ventricle was simplified radically and approximated by a half ellipsoid (Fig. 1d) with circular cross-section, characterised by the length h, short axis radius r and mural thickness s, varying accordingly from base to apex. The half axes of the epicardial surface had a relation 1:2 while the ones of the endocardium were in the ratio 1:3. In the resulting prolate spheroidal geometry, we introduced an FE mesh consisting of some 11 700 elements.

To further study the impact of the chosen characteristic parameters h, r and s on cardiac function, we rescaled the adjusted prolate spheroid in its long and short axes, respectively, in various steps. The end-diastolic volume therefore changed.

3. Results

3.1. Variations in alignment of the aggregated myocytes

The model shown in Fig. 1a, which provides realistic values for mural thickening, longitudinal and circumferential shortening, twisting as well as stroke volume [14], served as a baseline for comparison. With respect to the angle of intrusion, the largest effect of the variations described by transformations $\mathbf{\Phi}$ ($-14^\circ \le \phi \le 0^\circ$ and $0^\circ \le \phi \le 14^\circ$, $\Delta\phi = \pm 2^\circ$) was found for negative angles of rotation ϕ, in other words, for aggregates intruding from endocardium to epicardium, regardless of their helical orientation in that the stroke volume of the left ventricle decreased steadily from the maximum of 71 ml (baseline, i.e., $\phi = 0^\circ$ with end-diastolic volume 118 ml and end-systolic 47 ml) to 65.5 ml for $\phi = -14^\circ$. For deviations from the original orientation of the aggregates in a positive direction, in turn, the stroke volume decreased to a lesser extent such that, for $\phi = 14^\circ$, it reached a value of 68.6 ml.

In Fig. 2, we show colour-coded maps of calculated von Mises equivalent stress and strain in a septal–lateral long-axis section at the end-systole for $\phi = 14^\circ$, $\phi = 0^\circ$ and $\phi = -14^\circ$. We found that small alterations of $\phi = \pm 4^\circ$ from the original angles of intrusion, which already include a substantial amount of deviation from a tangential direction, did not change the patterns of stress or strain markedly. Even larger positive values ($\phi = 14^\circ$) merely changed the global pattern of deformation and the distribution of stress and strain. Negative changes of the intruding angle affected the global deformation pattern and the stress–strain distribution more effectively (Fig. 2e and f: $\phi = -14^\circ$); however, even in this case, the changes of the transmural variation of stress and strain were not large. To make a qualitative comparison, we calculated radial (E_{RR}), circumferential (E_{CC}) and longitudinal (E_{LL}) strains in basal, equatorial and apical areas from epicardium to endocardium. In Figs. 3–5, we show the transmural variations of the normal strains at septal, anterior, lateral and inferior walls of the basal section for $\phi = 14^\circ$, $\phi = 0^\circ$ and $\phi = -14^\circ$, respectively. In each area, for all values of ϕ, the same path of nodes was followed, so that the changes in the curves reflect only the variation in the angle of rotation, ϕ.

When using the original orientation field, calculation of longitudinal shortening from apex to base at septal, anterior, lateral and inferior sides showed that such shortening is practically equal around the ventricle. This is in agreement with recent experimental measurements [7,20]. Small changes in the angle of intrusion of the aggregated myocytes from their original orientation ($-4^\circ \le \phi \le 4^\circ$) did not change this pattern remarkably, while larger changes in values ($\phi = \pm 14^\circ$) affected the shortening only moderately, by up to 2%. According to experimental measurements [21], the twisting of the ventricular mass is counter clockwise when viewed from the apex, and irregularly distributed from the base to the apex on the endocardial and epicardial surfaces. It increases between basal and apical levels from the epicardium, at about 10°, to the endocardium, where it approximates 14°. In our simulations, twisting was counter clockwise as viewed from the apex, and reached about 10° on the epicardial wall. Changes in the angle of intrusion of $-14^\circ \le \phi \le 14^\circ$ did not significantly affect this pattern, nor the value of twisting.

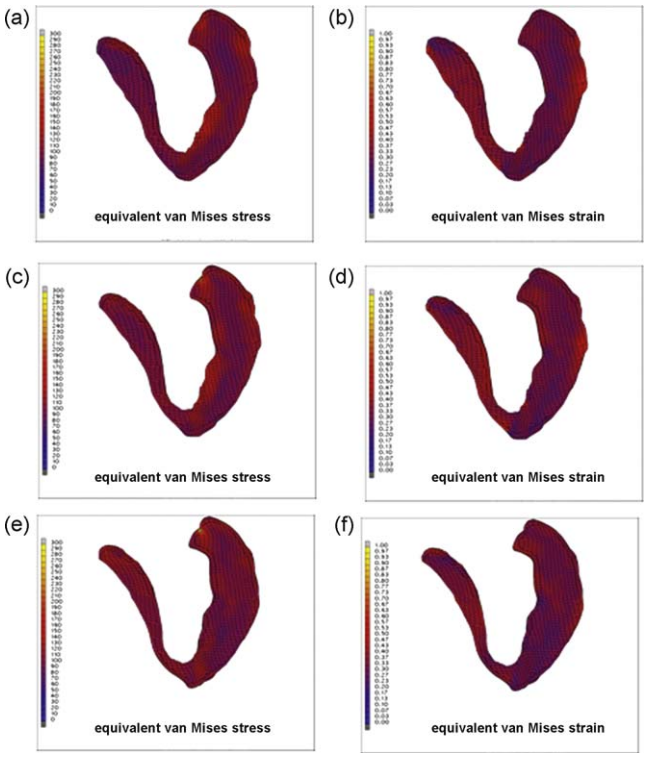

Fig. 2. Colour-coded maps of von Mises equivalent stress (left, in kPa) and strain (right) for a slice of elements in septal–lateral cross-section for $\phi = 14^\circ$ (a, b), $\phi = 0^\circ$ (c, d) and $\phi = 14^\circ$ (e, f), respectively.

The impact of changes in the helical angle of the aggregated myocytes, that is, transformations $\mathbf{\Theta}$, produced small variations: for $-14^\circ \le \theta \le 0^\circ$, the ventricular stroke volume decreased steadily from the original value of 71 ml at 0° to 69.9 ml for $\theta = -14^\circ$. For positive changes, the stroke volume was almost constant. The transmural variation of radial (E_{RR}), circumferential (E_{CC}) and longitudinal (E_{LL}) strains in the equatorial ventricular area from epicardium to endocardium for θ in the interval $\pm 14^\circ$ did not change markedly (not shown here for brevity). Similarly, changes in longitudinal shortening at different sides around the ventricle were small, up to 2%, and twisting was unaffected.

Downloaded from https://academic.oup.com/ejcts/article/37/2/384/775894 by guest on 25 April 2024

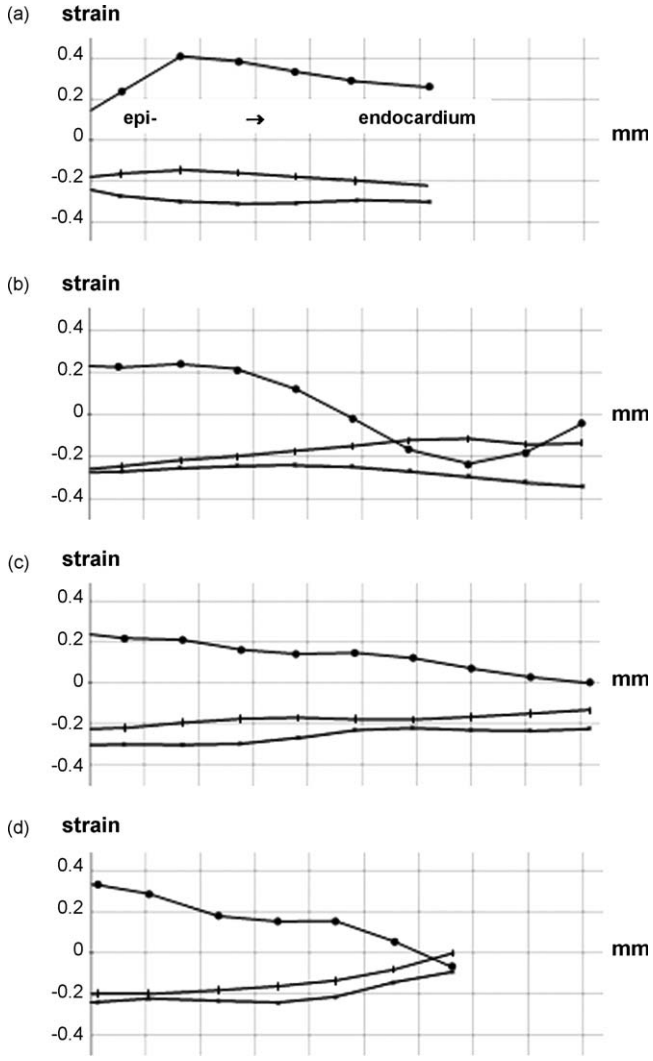

Fig. 3. Radial (●, E_{RR}), circumferential (‖, E_{CC}) and longitudinal (*, E_{LL}) components of strain in the (a) septal, (b) anterior, (c) lateral and (d) inferior wall of the basal area for the case $\phi = 14^\circ$. Depicted are the strain values for a representative chain of FE nodes from the epicardium (left) to the endocardium (right). The nodes were chosen in radial direction, but they do not necessarily follow a straight line. The sequence of nodal points is depicted along the abscissa according to their cumulative distance from the epicardium, before onset of simulated contraction (node-to-node distances in mm).

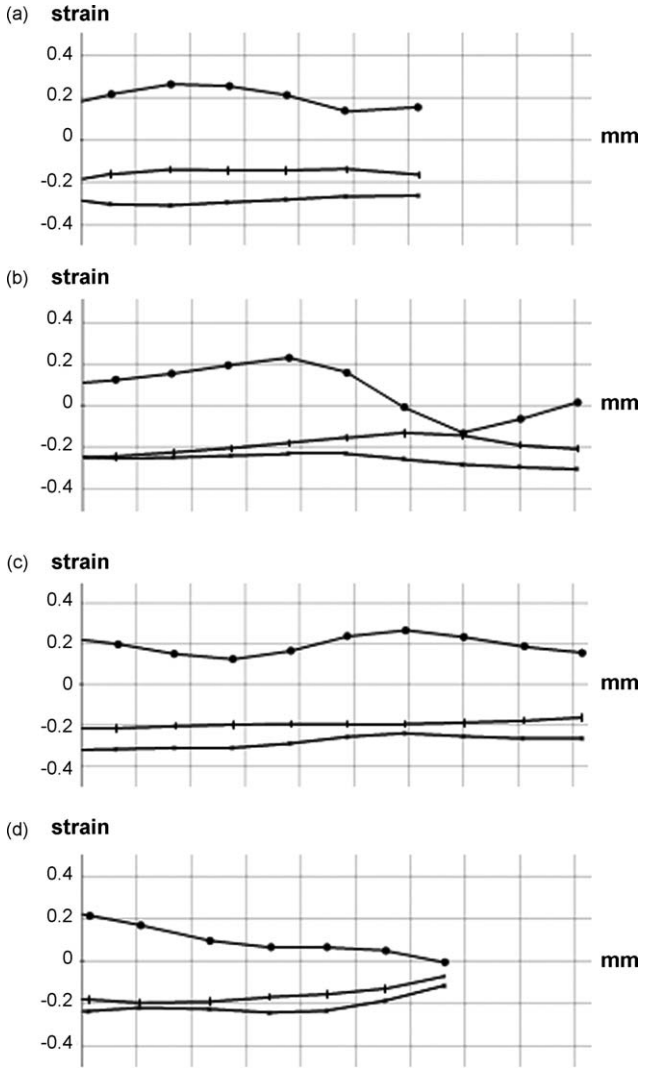

Fig. 4. Radial (●, E_{RR}), circumferential (‖, E_{CC}) and longitudinal (*, E_{LL}) components of strain in the (a) septal, (b) anterior, (c) lateral and (d) inferior wall of the basal area from epicardium (left) to endocardium (right) for the case $\phi = 0^\circ$. The abscissa is defined as in Fig. 3.

Rotations around the direction of orthotropy, given by transformation $\mathbf{\Omega}$ ($-14^\circ \leq \omega \leq 14^\circ$), again revealed little sensitivity: the left ventricular stroke volume decreased steadily from the original value of 71 ml at $\omega = 0^\circ$ to 68.7 ml for $\omega = -14^\circ$ and to 69.8 ml for $\omega = 14^\circ$. No significant change resulted in patterns of either stress or strain throughout the wall. Similar results were found for longitudinal shortening at septal, anterior, lateral and inferior sides of the ventricle, as well as for twisting.

3.2. Conformational changes

For both modified geometries (Fig. 1c and d), we followed the same approach, as described previously, of rotating the local coordinate system in each element up to $\pm 14^\circ$ in steps of 2° around all three local axes. We calculated the ventricular volume at end-systole, and also longitudinal shortening around the ventricle. Results were not essentially different from those described above, in that for transformations $\mathbf{\Theta}$ and $\mathbf{\Omega}$, both the modified models showed a similar behaviour, with small changes in the distribution of the equivalent von Mises stress and strain as well as of the radial (E_{RR}), circumferential (E_{CC}) and longitudinal (E_{LL}) strains in basal, equatorial and apical ventricular sections from epicardium to endocardium. Moreover, for transformation $\mathbf{\Phi}$, both the models exhibited again a maximal change of stroke volume. While for the realistic geometry (Fig. 1a), the maximal stoke volume occurred at $\phi = 0^\circ$, in case of the truncated geometry (Fig. 1c), this maximum was reached at $\phi = 2^\circ$ and for the adjusted spheroidal geometry (Fig. 1d) at $\phi = 6^\circ$.

Large variations of geometry were also considered for the adjusted prolate spheroidal model. Cutting down the length from h to $0.5h$ caused the ejection fraction to decrease by about 10%, whereas upon increasing the length from h to $2h$,

Downloaded from https://academic.oup.com/ejcts/article/37/2/384/775894 by guest on 25 April 2024

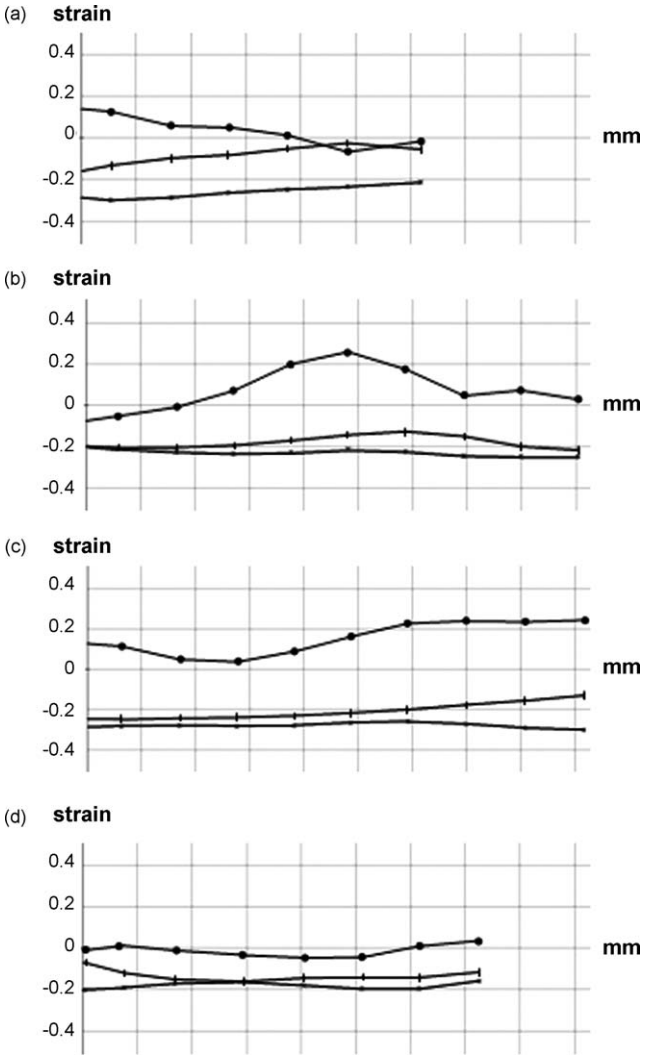

Fig. 5. Radial (●, E_{RR}), circumferential (▮, E_{CC}) and longitudinal (*, E_{LL}) components of strain in the (a) septal, (b) anterior, (c) lateral and (d) inferior wall of the basal area from epicardium (left) to endocardium (right) for the case $\phi = -14^{\circ}$. The abscissa is defined as in Fig. 3.

the ejection fraction was augmented by about 5%. Doubling the mural thickness from s to $2s$ increased the ejection fraction by about 12%. Decreasing the left ventricular radius from r to $0.5r$ augmented the ejection fraction by more than 17%. In both the cases, improvement of ejection fraction was caused by an increase of mural thickening.

3.3. Large variations in the alignment of the aggregated myocytes

We then studied the impact of a more pronounced intrusion angle of the myocytes, whereby the transformations of Φ proved to be very sensitive, as found previously. Using the same procedure as described before, systolic contraction was simulated systematically for reorientations in the interval $0^{\circ} \leq \phi \leq 90^{\circ}$. The typical dependence of stroke volume on this angle, between 0° and 45°, is shown in Fig. 6. It is seen that, for angles greater than 30°, the stroke volume decreases significantly, reaching zero at 45°. This can

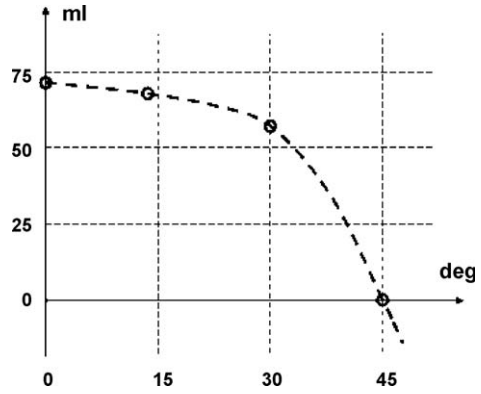

Fig. 6. Typical dependence of stroke volume, in ml, on deviation from original orientations of the myocytes, in degrees. Note that all strands of aggregated myocytes in the ventricular walls are subjected to the same deviation in terms of rotation from their original direction towards the endocardium. For definitions, see the text.

readily be explained: whenever the average direction deviates by an amount of more than 45° from a surface-parallel direction, contraction must counteract ejection, producing mural thinning. Accordingly, the stroke volume becomes formally negative. At 45°, contraction has no effect on mural thickness. Twisting still prevails such that there is still some change in ventricular volume, although not shown in the schematic sketch (Fig. 6).

4. Discussion

During the past two decades, innovative cardiac surgeons have established new techniques that challenge earlier standards. The community of cardiac surgeons as a whole, however, remains divided with respect to the validity of these techniques for remodelling ventricular size and shape. While one group championed the need to restore the elliptic ventricular shape deemed to be optimal for normal function [13,22], others placed greater emphasis on the known vulnerability of the myocardium [23]. In particular, Batista [24] suggested that the mere reduction in left ventricular radius achieved by resecting part of the wall would prove to be an efficient way of restoring the function of a dilated left ventricle. Common to surgical procedures affecting myocardial mass and geometry is a reorientation of the myocardial fibre trajectories.

Our main purpose in this study, therefore, was to focus on the influence on stroke volume of the orientation of the myocytes aggregated together within the left ventricular wall. Earlier models seeking to relate ventricular structure to function have been based on the notion that myocardial contraction essentially produces ventricular emptying. Because of this presumption, forces acting in non-concentric direction have largely been excluded from consideration. Yet, if the models are to be of clinical relevance, they must include established details concerning ventricular anatomy. We based our own model, therefore, on a realistic alignment of the myocardial meshwork as demonstrated by peeling the myocytes in the walls of the human left ventricle.

Downloaded from https://academic.oup.com/ejcts/article/37/2/384/775894 by guest on 25 April 2024

The simulations showed that the overall performance of a real heart exhibits remarkable stability with respect to changes of the local myocytic architecture. This fact has significance for the surgical procedures mentioned above, in that it confirms notions that ventricular size and shape can be reduced and rhythms synchronised by using surgical and electrophysiological tools. In consideration of the marked structural remodelling induced in any diseased heart as it seeks to sustain an adequate pump function, it has been our opinion that moderate changes of the global myocardial architecture would not exhibit any significant influence on ventricular function as long as there is minimal ischaemia or fibrosis, and the electrical conduction system remains functional. Our simulations have now validated this premise.

We conclude that our findings are hardly compatible with the notion that the ventricular walls are composed of extended discrete bands, or tracts – concepts that remain popular for some who seek to explain cardiodynamics [12,13]. Our data obtained while systematically modulating ventricular geometry rather show that, for each left ventricular conformation, there is an optimal arrangement of the aggregated myocytes, which is associated with the production of a maximal stroke volume. This optimal structure behaves in a robust fashion, given that moderate modulations in the orientation of the aggregated myocytes do not significantly change the distributions of stress and strain, apart from some small regions on the epicardial and endocardial surfaces produced by pre-existing superficial irregularities. When changing the orientation of the myocytes, we purposely used small-to-moderate increments relative to tangential orientation. The maximum value used was 14°, this value being near to the range of greatest angulation measured in the normal heart by Streeter and his colleagues [1]. Larger changes in the angulations, of 30° and more, however, produced significant changes in cardiodynamics. Whenever the angle of intrusion exceeds 45°, which, in reality, is observed only in restricted areas around the anchorage of the papillary muscles, mural contraction counteracts systolic thickening. If a major population of aggregated myocytes was assumed to have an essentially radial orientation, the stroke volume would become negative, with the ventricle being larger after systolic contraction. We confirmed this assumption when we imposed uniformly an angle of intrusion of greater than 45°.

The only theoretical studies known to us that have studied the effect of variations of the orientation field on left ventricular function are those performed by Bovendeerd and his colleagues [25] These authors presumed a symmetrical spheroidal geometry and a homogeneous surface-parallel alignment of myocytes. They found a sensitive dependence of the distributions of strain and stress, and of the stroke volume, on the orientation field. Our results are not in agreement with this work. We believe that the most important reason for this difference derives from the assumptions made regarding the orientation of the myocytes. A completely ordered and homogeneous orientation field parallel to the surface must be expected to be mechanically sensitive to any change. In contrast, an orientation field with local inhomogeneity, and with a spectrum of intruding angles, is insensitive to small-to-moderate deviations or some disarray, of the aggregated myocytes. Such structural heterogeneity provides a robust structure. According to Brutsaert [11], a certain degree of structural and functional heterogeneity is an important prerequisite for regulation of ventricular mural function.

Our results show that, while attempting to improve cardiac function at a given alignment of aggregated myocytes, it is the left ventricular dimensions that need to be adjusted. At the same setting of the active stress tensor, any changes in ventricular geometry produced by increasing s or decreasing r mediated significant deformations. We conclude, therefore, that reduction of ventricular dimensions augments the ejection fraction and, at the same time, diminishes the active stress tensor. This purely mechanical aspect of cardiac function is in agreement with the basic concept of partial left ventriculectomy as described by Batista [24]. Our model supports this assumption that, in properly selected cases, the major effect is that of a reduction in ventricular radius associated with a concomitant increase in mural thickness.

We recognise, nonetheless, that our modelling includes a number of significant approximations and suffers from three major limitations. First, we have considered only uniform changes in the overall alignment of the aggregated myocytes. In reality, there are wide variations in the alignments between ventricular regions, particularly in the setting of cardiac disease. Second, we have not considered the influence of the collageneous matrix, the vascular system and of eventual submicroscopic structural characteristics of the myocardium. Yet, mural fibrosis tends to develop at the early stages of cardiac disease. As such fibrosis develops, deteriorating pump function relates not only to alterations in myocytic alignments, but also to their fettering by the matrix, and to the associated deviation of contractile forces from the tangential to the radial direction. Third, it is well established that the alignment of the myocytes is disturbed in certain pathologic processes such as hypertrophic cardiomyopathy. Our model can only partially be used for such diseases, as we investigated only uniform variations in the alignment of the myocytes. Further, minor limitations derive from our disregard of residual wall stresses, as well as intracavitary pressure gradients. Both effects, however, have a small influence on systolic wall stresses.

In conclusion, our model shows that the heart maintains a remarkably stable function despite simulated disorders in the orientation of the myocytes aggregated within the ventricular walls. We attribute this finding to the fact that, already in a healthy heart, there is a local inhomogeneous pattern of the alignment of the myocytes in the ventricular walls. Such regional heterogeneity is, therefore, overlaid on the global systemic alignment, providing a stabilising effect with respect to ventricular function. Our results strongly support the concept that the ventricular walls are made up of a homogeneous and continuous 3D myocardial mesh, lacking any discrete anatomical subcomponents exhibiting mechanical functionality such as ventricle-wide tracts, or bands, which could be destroyed surgically.

Downloaded from https://academic.oup.com/ejcts/article/37/2/384/775894 by guest on 25 April 2024

References

[1] Streeter Jr DD. Gross morphology and fiber geometry of the heart. In: Berne RM, editor. Handbook of physiology. Baltimore: Williams & Wilkins; 1979.
[2] Greenbaum RA, Ho SY, Gibson DG, Becker AE, Anderson RH. Left ventricular fibre architecture in man. Brit Heart J 1981;45:248—63.
[3] Sanchez-Quintana D, Garcia Martinez V, Hurle JM. Myocardial fibre architecture in the human heart. Acta Anat 1990;138:352—8.
[4] LeGrice IJ, Takayama Y, Covell JW. Transverse shear along myocardial cleavage planes provides a mechanism for normal systolic wall thickening. Circ Res 1995;77:182—93.
[5] Dorri F, Niederer PF, Redmann K, Lunkenheimer PP, Cryer CW, Anderson RH. An analysis of the spatial arrangement of the myocardial aggregates making up the wall of the human left ventricle. Eur J Cardio-thoracic Surg 2007;31:430—7.
[6] MacGowan GA, Shapiro EP, Azhari H, Siu CO, Hees PS, Hutchins GM, Weiss JL, Rademakers FE. Non-invasive measurement of shortening in the fiber and cross-fiber directions in the normal human left ventricle and in idiopathic dilated cardiomyopathy. Circulation 1997;96:535—41.
[7] Rademakers FE, Rogers WJ, Guier WH, Hutchins GM, Siu CO, Weisfeldt ML, Weiss JL, Shapiro EP. Relation of regional cross-fiber shortening to wall thickening in the intact heart. Three-dimensional strain analysis by NMR tagging. Circulation 1994;89:1174—82.
[8] Lunkenheimer PP, Redmann K, Dietl K-H, Cryer C, Richter K-D, Whimster WF, Niederer P. The heart's fibre alignment assessed by comparing two digitizing systems. Methodological investigation into the inclination angle toward wall thickness. Technol Health Care 1997;5:65—77.
[9] Lunkenheimer PP, Redmann K, Florek J, Fassnacht U, Cryer CW, Wübbeling F, Niederer P, Anderson RH. The forces generated within the musculature of the left ventricular wall. Heart 2004;90:200—7.
[10] Arts T, Prinzen FW, Snoeckx LHEH, Rijcken JM, Reneman RS. Adaptation of cardiac structure by mechanical feedback in the environment of the cell: a model study. Biophys J 1994;66:953—61.
[11] Brutsaert DL. Nonuniformity: a physiologic modulator of contraction and relaxation of the normal heart. J Am Coll Cardiol 1987;9:341—8.
[12] Torrent-Guasp F, Kocica MJ, Corno AF, Komeda M, Carreras-Costa F, Flotats A, Cosin-Aguillar J, Wen H. Towards new understanding of the heart structure and function. Eur J Cardio-thoracic Surg 2005;27:101—201.
[13] Buckberg G, Hoffmann JIE, Mahajan A, Saleh S, Coghlan C. Cardiac mechanics revisited: the relationship of cardiac architecture to ventricular function. Circulation 2008;118:2571—87.
[14] Dorri F, Niederer PF, Lunkenheimer PP. A finite element model of the human left ventricular systole. Comput Methods Biomech Biomed Eng 2006;9:319—41.
[15] Lin DHS, Yin FC. A multiaxial constitutive law for mammalian left ventricular myocardium in steady-state barium contracture or tetanus. J Biomech Eng 1998;120:504—17.
[16] Yin FC, Chan CC, Judd RM. Compressibility of perfused passive myocardium. Am J Physiol Heart Circ Physiol 1996;40:H1864—70.
[17] Nash MP, Hunter PJ. Computational mechanics of the heart. J Elasticity 2000;61:113—41.
[18] Novak VP, Yin FC, Humphrey JD. Regional mechanical properties of passive myocardium. J Biomech 1994;27:403—12.
[19] Humphrey JD, Strumpf RK, Yin FC. Determination of a constitutive relation for passive myocardium: II. Parameter estimation. J Biomech Eng 1990;112:340—6.
[20] Petitjean C, Rougon N, Cluzel P. Assessment of myocardial function: a review of quantification methods and results using tagged MRI. J Cardiovasc Magn Reson 2005;7:501—16.
[21] Moore CC, Lugo-Olivieri CH, McVeigh ER, Zerhouni EA. Three-dimensional systolic strain patterns in the normal human left ventricle: characterization with tagged MR imaging. Radiology 2000;214:453—66.
[22] Athanasuleas CL, Buckberg GD, Stanley AWH, Siler W, Dor V, Di Donato M, Menicanti L, de Oliveira SA, Beyersdorf F, Kron IL, Suma H, Kouchoukos N, Moore W, McCarthy PM, Oz MC, Fontan F, Scott ML, Accola KA. Surgical ventricular restoration: The RESTORE group experience. Heart Fail Rev 2005;9:287—97.
[23] Birdi I, Bryan A, Angelini G. Detection and prevention of myocardial damage during open heart surgery. Heart 1996;76:189—90.
[24] Westaby S, Batista R, Mohr FW, Pattakos E. Partial left ventriculectomy—the Batista procedure. Eur J Cardio-thoracic Surg 1999;15:S12—9.
[25] Bovendeerd PH, Huyghe JM, Arts T, van Campen DH, Reneman RS. Influence of endocardial—epicardial crossover of muscle fibers on left ventricular wall mechanics. J Biomech 1994;27:941—51.

Downloaded from https://academic.oup.com/ejcts/article/37/2/384/775894 by guest on 25 April 2024